

## The effect of absorber doping on electrical and optical properties of nBn based type-II InAs/GaSb strained layer superlattice infrared detectors

Stephen Myers,<sup>1</sup> Elena Plis,<sup>1</sup> Arezou Khoshakhlagh,<sup>1</sup> Ha Sul Kim,<sup>1</sup> Yagya Sharma,<sup>1</sup> Ralph Dawson,<sup>1</sup> Sanjay Krishna,<sup>1,a)</sup> and Aaron Gin<sup>2</sup>

<sup>1</sup>Department of Electrical and Computer Engineering, Center for High Technology Materials, University of New Mexico, Albuquerque, New Mexico 87106, USA

<sup>2</sup>Center for Integrated Nanotechnologies, Sandia National Laboratories, P.O. Box 5800, Albuquerque, New Mexico 87185-1303, USA

(Received 17 July 2009; accepted 21 August 2009; published online 24 September 2009)

We have investigated the electrical and optical properties of a nBn based InAs/GaSb strained layer superlattice detector as a function of absorber region background carrier concentration. Temperature dependent dark current, responsivity, and detectivity were measured. The device with a nonintentionally doped absorption region demonstrated the lowest dark current density with a specific detectivity at zero bias equal to  $1.2 \times 10^{11}$  cm Hz<sup>1/2</sup>/W at 77 K. This value decreased to  $6 \times 10^{10}$  cm Hz<sup>1/2</sup>/W at 150 K. This contrasts significantly with *p-i-n* diodes, in which the  $D^*$  decreases by over two orders of magnitude from 77 to 150 K, making nBn devices promising for higher operating temperatures. © 2009 American Institute of Physics. [doi:10.1063/1.3230069]

Infrared (IR) detectors have a broad range of applications in civilian, medical, industrial, astronomical, and military fields. The technologies currently dominating the IR detector market (3–12 μm) are mercury cadmium telluride (MCT), indium antimonide (InSb), and quantum well infrared photodetectors (QWIP). However, lack of spatial uniformity over a large area and low yield for large focal plane arrays (FPAs) still plague MCT<sup>1</sup> devices. While InSb detectors dominate the mid wave infrared (MWIR, 3–5 μm) regime, their wavelength response is not tailorable due to a fixed bandgap and the devices are limited to cryogenic temperatures.<sup>2</sup> The QWIPs are based on a mature GaAs technology and demonstrate very good uniformity and reproducibility. However they have large dark currents and low quantum efficiencies compared to interband devices. The type-II strained layer superlattice (SLS) material system was first theoretically proposed by Tsu *et al.*<sup>3</sup> in 1977. A decade later Smith and Mailhot<sup>4</sup> demonstrated that the optical absorption for the InAs/(In,Ga)Sb SLS material is as good as the MCT alloy with the same bandgap. Since then the SLS material has generated significant interest in IR detection.

The InAs/GaSb SLS is characterized by a so called “broken-gap” type-II alignment, with the conduction band edge of InAs located lower than the valence band edge of GaSb. Spatially indirect optical transitions between holes localized in GaSb layers and electrons confined in InAs layers are employed for the detection of infrared radiation. By varying the composition and thickness of constituent layers, the effective bandgap of an InAs/GaSb detector can be tuned between 3 and 30 μm. The SLS is characterized by reduced Auger recombination rates due to the spatial separation of electrons and holes.<sup>5</sup> In contrast with QWIPs,<sup>6</sup> normal incidence absorption is permitted in SLS resulting in high quantum efficiency. In addition, the electron effective mass is not dependent on the bandgap size and is larger than that measured in MCT detectors<sup>7</sup> which leads to reduced tunneling

currents. Commercial availability of low defect density substrates and a high degree of uniformity for III-V processing over a large area also offers technological advantages for the SLS. This makes detectors based on SLs an attractive technology for realization of high performance single element detectors and FPAs.<sup>8–13</sup>

Presently most SLS detectors are based on a photodiode (*p-on-n* or *n-on-p*) design. In this case, two main contributions to dark current are surface leakage currents associated with the mesa sidewall exposure, which defines the device optical area, and generation-recombination current associated with Shockley–Read–Hall (SRH) centers in the depletion region of the photodiode. With scaling of device dimensions (typical dimensions of an FPA pixel is  $\sim 20 \times 20$  μm<sup>2</sup>), the surface/volume ratio is increased and detector performance is strongly dependent on surface effects. In order to overcome the limitation imposed by surface leakage currents, a stable surface passivation layer is needed. Various research groups have developed different passivation and coating processes that are stable, insensitive to the device cutoff wavelength and easily integrated into fabrication processes.<sup>14–17</sup>

The nBn detector structure was recently proposed<sup>18</sup> which utilizes both a wide-bandgap barrier to block majority carriers and a buried, planar device structure effectively eliminating surface currents. In addition, it excludes the SRH generation-recombination component of dark current since it is intended to operate with *n*-type layers in flatband or with little depletion. The typical SLS photodetector with an nBn design is formed by a nonintentionally doped (NID) thick SLS absorber layer grown on the top of a *n*-type bottom contact layer, followed by a 100 nm barrier layer and capped by a thin *n*-type contact layer.<sup>19,20</sup> Due to a nearly zero valence band offset and a large conduction band offset, the majority carrier current between the two electrodes is blocked, while photogenerated minority carriers do not see a barrier. Due to processing utilized for nBn detectors, the size of the device, unlike a conventional photodiode, is not defined by the dimensions of the etched mesa but by the lateral

<sup>a)</sup>Author to whom correspondence should be addressed. Electronic mail: skrishna@chtm.unm.edu.

diffusion length of minority carriers (holes). The second recently proposed approach for realization of room temperature detectors utilizes heavy hole/light hole to split-off transitions. With this design a  $D^*$  of  $6.8 \times 10^5$  Jones at  $2.5 \mu\text{m}$  operating at 300 K has been achieved.<sup>21</sup>

It is well known that for the design of narrow bandgap photodiodes the doping level in the absorber regions is a very important parameter that affects the electrical and optical performance of the device.<sup>22</sup> However, the effect of the absorber doping on nBn devices has not been studied before. In this paper, we have investigated the electrical and optical properties of an nBn based InAs/GaSb SLS MWIR detector as a function of background carrier concentration of the absorber. Temperature-dependent dark current, responsivity, and detectivity of the nBn MWIR detector as a function of absorber doping were measured.

The detector structures were grown on *n*-type (Te-doped) GaSb (100) epitaxial substrates using solid source molecular beam epitaxy in a VG-80 system equipped with valved cracker sources for group V  $\text{Sb}_2$  and  $\text{As}_2$  fluxes and Ga/In SUMO<sup>®</sup> cells. Growth details have been reported elsewhere.<sup>23</sup> The device structure consists of a  $\sim 1 \mu\text{m}$  10 monolayers (MLs) InAs/10 MLs GaSb SLS (170 periods) absorber grown on top of a  $\sim 0.36 \mu\text{m}$  thick *n*-type contact layer (composed of the SLS with the same composition and thickness but with Si-doped InAs layers). This was followed by a 100 nm  $\text{Al}_{0.2}\text{Ga}_{0.8}\text{Sb}$  NID (*p*-type) barrier layer and a 20 nm GaSb NID spacer layer. The structure was capped by a  $\sim 0.1 \mu\text{m}$  thick top contact layer with the same superlattice composition, thickness, and doping concentration as the bottom contact layer. The doping concentration of the absorbing region was equal to  $5 \times 10^{16} \text{ cm}^{-3}$  (NID SLS material),  $1.4 \times 10^{17} \text{ cm}^{-3}$ ,  $4.0 \times 10^{17} \text{ cm}^{-3}$ , and  $3.5 \times 10^{18} \text{ cm}^{-3}$  as determined from Hall measurements on samples grown on GaAs substrates. The material was processed into normal incidence single-pixel detectors with  $410 \mu\text{m} \times 410 \mu\text{m}$  mesas with apertures varying from 25 to  $300 \mu\text{m}$  in diameter using standard optical photolithography and dry etching techniques.

The spectral response of the detectors was measured with a Nicolet 670 Fourier transform infrared spectrometer relative to a standard deuterated triglycine sulfate thermal detector. The 100%-cut-off wavelength of the NID detector is equal  $\sim 6 \mu\text{m}$  whereas the detector with the largest doping level ( $n=3.5 \times 10^{18} \text{ cm}^{-3}$ ) shows a 100% cutoff wavelength at  $\sim 4.5 \mu\text{m}$ . The observed blueshift of cutoff wavelength is attributed to the Moss–Burstein effect. Absolute comparison of the response of the four detectors measured at  $T=77 \text{ K}$  with a bias of  $V_b=0.1 \text{ V}$  is presented in Fig. 1.

Current-voltage (*IV*) characteristics were measured for the devices at 77 K using a HP4145 semiconductor parameter analyzer as shown in Fig. 2. It should be noted that the forward bias is defined as a positive voltage applied to the bottom contact of the device. At 77 K and 0.1 V of applied bias, the dark current density increases by three orders of magnitude (from  $\sim 0.3 \text{ mA/cm}^2$  to  $\sim 0.3 \text{ A/cm}^2$ ), when the doping concentration is changed from  $5 \times 10^{16}$  to  $3.5 \times 10^{18} \text{ cm}^{-3}$ . The observed increase in dark current density of the nBn detector with increased doping of the absorption region contradicts our expectations. Since the nBn detector is designed to operate as a minority (hole) carrier photoconductor device in flatband conditions, the *n*-type doping level of

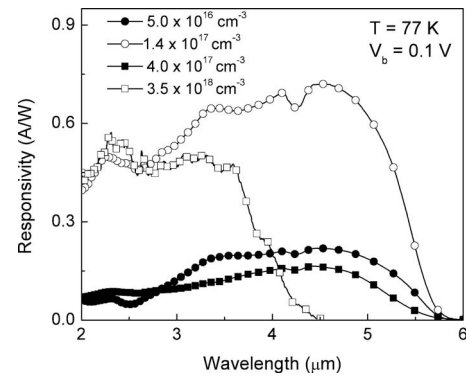


FIG. 1. Responsivity of the four detectors with doping concentrations of  $5.0 \times 10^{16}$  (NID),  $1.4 \times 10^{17}$ ,  $4.0 \times 10^{17}$ , and  $3.5 \times 10^{18} \text{ cm}^{-3}$  at  $T=77 \text{ K}$  with a bias of  $V_b=0.1 \text{ V}$ .

the absorbing region is not supposed to influence device operation.<sup>24</sup> For a conventional photodiode, the increase of absorber doping above  $10^{16} \text{ cm}^{-3}$  would result in a very thin depletion region and Zener breakdown,<sup>24</sup> which is not the case for the unipolar nBn detector device. We believe that this increase in the dark current suggests that there is a quantum well (QW) for the minority carriers (holes) formed in the valence band. With an increase in the doping level of the absorber the depth of this QW increases. We think, during the device operation holes may be trapped in the QW whereas electrons are accumulated near the barrier. This leads to an enhanced electron-hole recombination. Thus, for the higher doped absorber region the carrier lifetime will be decreased due to the increase in electron-hole recombination. Since dark current is inversely proportional to the carrier lifetime, the increase in dark current density is expected and observed for the higher doped devices.

Specific detectivity ( $D^*$ ) was estimated using the following equation:

$$D^* = R_\lambda \sqrt{2qJ + (4kT)/(R_d A_d)}, \quad (1)$$

where  $R_\lambda$  is the responsivity,  $q$  is the electronic charge,  $J$  is the dark current density,  $k$  is the Boltzmann constant,  $T$  is the temperature of the device,  $R_d$  is the dynamic resistance, and  $A_d$  is the diode area. The  $D^*$  was calculated at  $4.4 \mu\text{m}$  for all studied detectors.

The responsivity was measured using a Stanford Research SR770 FFT network analyzer and a Mikron blackbody set to  $800 \text{ }^\circ\text{C}$ . At 150 K, responsivity reached  $1 \text{ A/W}$  at zero bias.

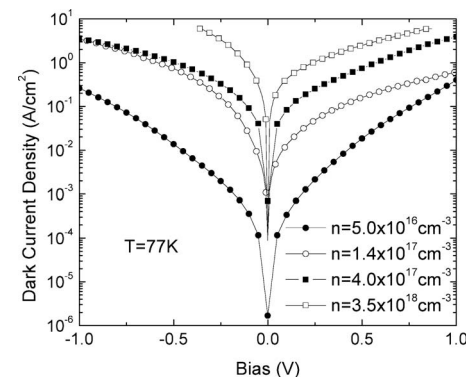


FIG. 2. Dark current density vs applied bias of the detectors with four different doping concentrations at 77 K.

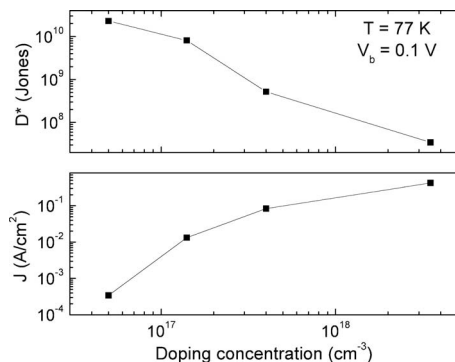


FIG. 3. Specific detectivity and dark current density as a function of doping concentration in absorption region of nBn MWIR detector ( $V_b=0.1$  V and  $T=77$  K).

The low-temperature (77 K) dependencies of specific detectivity along with the dark current density as a function of  $n$ -type doping level of the absorption region are presented in Fig. 3 ( $V_b=0.1$  V). The significant degradation of both parameters with increased  $n$ -type doping level of the absorbing region is observed. The maximum detectivity that was measured was  $2.3 \times 10^{10}$  Jones for the NID device (0.1 V). The bias-dependent values of  $D^*$  at 77 K for the four devices are shown in Fig. 4.

The temperature dependence of  $D^*$  for the NID detector was also investigated. The zero bias  $D^*$  was estimated to be  $6 \times 10^{10}$  Jones at 150 K for the NID device, which is comparable with state-of-the-art  $p$ - $i$ - $n$  diodes at the same operating temperature.<sup>25</sup> At 0.1 V of applied bias,  $D^*$  was found to be  $\sim 1.6 \times 10^{10}$  Jones. Thus, no significant degradation of  $D^*$  within (0–100) mV bias range with temperature was observed and the corresponding change in dark current density was less than an order of magnitude. For the  $p$ - $i$ - $n$  photodiode with nearly the same cut-off wavelength the  $D^*$  decreases by more than two orders of magnitude from 77 to 150 K<sup>25</sup> for the same bias range.

In conclusion, we have investigated the electrical and optical properties of a MWIR nBn detector as a function of background carrier concentration in the absorbing region of the device. Contrary to our expectations, dark current density was dramatically affected by the change of the  $n$ -type doping level in the detector absorption region. Such behavior can be

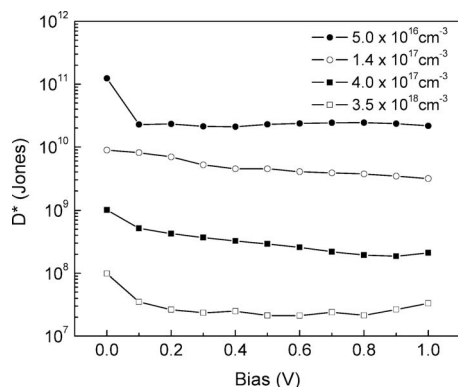


FIG. 4. Bias-dependent specific detectivity of the four detectors with doping concentrations of  $5.0 \times 10^{16}$  (NID),  $1.4 \times 10^{17}$ ,  $4.0 \times 10^{17}$ , and  $3.5 \times 10^{18}$   $\text{cm}^{-3}$  measured at  $T=77$  K.

attributed to the presence of a QW for the minority carriers (holes) formed in the valence band. The device with the NID doping level in the absorption region demonstrated the best performance among all studied samples with zero-bias values of current responsivity and specific detectivity equal to 1 A/W and  $6.0 \times 10^{10}$  Jones, respectively, (150 K) with a 0% cutoff near 6  $\mu\text{m}$ . The observed temperature dependence of  $D^*$  is significantly different from conventional  $p$ - $i$ - $n$  diodes, in which the  $D^*$  decreases by over two orders of magnitude from 77 to 150 K, making nBn devices a promising alternative for achieving higher operating temperatures.

The authors would like to acknowledge support from AFRL Contract No. FA9453-07-C-0171 and AFOSR Contract No. FA9550-09-1-0231. This work was performed, in part, at the Center for Integrated Nanotechnologies, a U.S. Department of Energy, Office of Basic Energy Sciences user facility. Sandia National Laboratories is a multiprogram laboratory operated by Sandia Corporation, a Lockheed-Martin Co., for the U.S. Department of Energy under Contract No. DE-AC04-94AL85000.

- <sup>1</sup>P. Norton, *Opto-Electron. Rev.* **10**, 159 (2002).
- <sup>2</sup>W. J. Parrish, J. D. Blackwell, R. C. Paulson, and H. Arnold, *Proc. SPIE* **1512**, 68 (1991).
- <sup>3</sup>G. A. Sai-Halasz, R. Tsu, and L. Esaki, *Appl. Phys. Lett.* **30**, 651 (1977).
- <sup>4</sup>D. L. Smith and C. Mailhot, *J. Appl. Phys.* **62**, 2545 (1987).
- <sup>5</sup>H. Mohseni, V. Litvinov, and M. Razeghi, *Phys. Rev. B* **58**, 15378 (1998).
- <sup>6</sup>B. F. Levine, *J. Appl. Phys.* **74**, R1 (1993).
- <sup>7</sup>A. Rogalski, *Opto-Electron. Rev.* **14**, 84 (2006).
- <sup>8</sup>E. Plis, J. B. Rodriguez, H. S. Kim, G. Bishop, Y. D. Sharma, L. R. Dawson, S. Krishna, S. J. Lee, C. E. Jones, and V. Gopal, *Appl. Phys. Lett.* **91**, 133512 (2007).
- <sup>9</sup>M. Razeghi, D. Hoffman, B.-M. Nguyen, P.-Y. Delaunay, E. K.-W. Huang, and M. Z. Tidrow, *Proc. SPIE* **6940**, 694009 (2008).
- <sup>10</sup>M. Walther, R. Rehm, J. Schmitz, F. Rutz, J. Fleissner, and J. Ziegler, *Proc. SPIE* **6940**, 69400A (2008).
- <sup>11</sup>B.-M. Nguyen, D. Hoffman, Y. Wei, P.-Y. Delaunay, A. Hood, and M. Razeghi, *Appl. Phys. Lett.* **90**, 231108 (2007).
- <sup>12</sup>J. Li, C. Hill, J. Mumolo, S. Gunapala, S. Mou, and S. Chuang, *Appl. Phys. Lett.* **93**, 163505 (2008).
- <sup>13</sup>I. Vurgaftman, E. Aifer, C. Canedy, J. Tischler, J. Meyer, J. Warner, E. Jackson, G. Hildebrandt, and G. Sullivan, *Appl. Phys. Lett.* **89**, 121114 (2006).
- <sup>14</sup>A. Gin, Y. Wei, A. Hood, A. Bajowala, V. Yazdanpanah, and M. Razeghi, *Appl. Phys. Lett.* **84**, 2037 (2004).
- <sup>15</sup>A. Hood, P.-Y. Delaunay, D. Hoffman, B.-M. Nguyen, Y. Wei, and M. Razeghi, *Appl. Phys. Lett.* **90**, 233513 (2007).
- <sup>16</sup>E. Plis, J. B. Rodriguez, S. J. Lee, and S. Krishna, *Electron. Lett.* **42**, 1248 (2006).
- <sup>17</sup>R. Rehm, M. Walther, F. Fuchs, J. Schmitz, and J. Fleissner, *Appl. Phys. Lett.* **86**, 173501 (2005).
- <sup>18</sup>S. Maimon and G. W. Wicks, *Appl. Phys. Lett.* **89**, 151109 (2006).
- <sup>19</sup>J. Rodriguez, E. Plis, G. Bishop, Y. D. Sharma, H. Kim, L. R. Dawson, and S. Krishna, *Appl. Phys. Lett.* **91**, 043514 (2007).
- <sup>20</sup>G. Bishop, E. Plis, J. B. Rodriguez, Y. D. Sharma, H. S. Kim, L. R. Dawson, and S. Krishna, *J. Vac. Sci. Technol. B* **26**, 1145 (2008).
- <sup>21</sup>P. V. V. Jayaweera, S. G. Matsik, A. G. U. Perera, H. C. Liu, M. Buchanan, and Z. R. Wasilewski, *Appl. Phys. Lett.* **93**, 021105 (2008).
- <sup>22</sup>D. Hoffman, B.-M. Nguyen, P.-Y. Delaunay, A. Hood, M. Razeghi, and J. Pellegrino, *Appl. Phys. Lett.* **91**, 143507 (2007).
- <sup>23</sup>E. Plis, S. Annamalai, K. T. Posani, S. Krishna, R. A. Rupani, and S. Ghosh, *J. Appl. Phys.* **100**, 014510 (2006).
- <sup>24</sup>P. Klipstein, *Proc. SPIE* **6940**, 69402U (2008).
- <sup>25</sup>Y. Wei, A. Hood, H. Yau, M. Razeghi, M. Z. Tidrow, and V. Nathan, *Appl. Phys. Lett.* **86**, 233106 (2005).